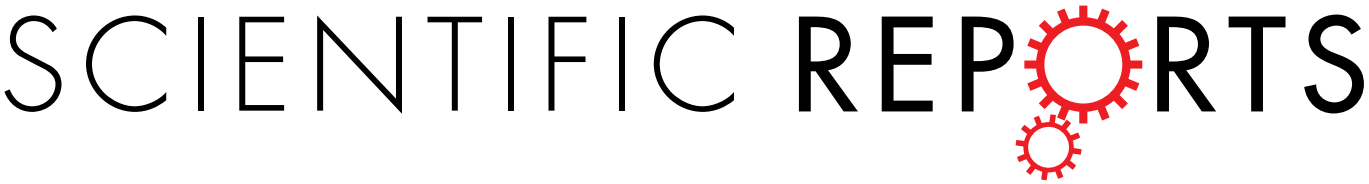

OPEN

Self-supporting Co_3O_4/Graphene Hybrid Films as Binder-free Anode Materials for Lithium Ion Batteries

Received: 21 November 2017
Accepted: 5 February 2018
Published online: 16 February 2018

Shouling Wang[3], Ronghua Wang[1], Jie Chang[3], Ning Hu[2] & Chaohe Xu[2,4]

A self-supporting Co_3O_4/graphene hybrid film has been constructed via vacuum filtration of $Co(OH)_2$ nanosheet and graphene, followed by a two-step thermal treatment. Within the hybrid film, Co_3O_4 nanoparticles with size of 40~60 nm uniformly *in-situ* grew on the surface of graphene, forming a novel porous and interleaved structure with strong interactions between Co_3O_4 nanoparticles and graphene. Such fascinating microstructures can greatly facilitate interfacial electron transportation and accommodate the volume changes upon Li ions insertion and extraction. Consequently, the binder-less hybrid film demonstrated extremely high reversible capacity (1287.7 mAh g^{-1} at 0.2 A g^{-1}), excellent cycling stability and rate capability (1110 and 800 mAh g^{-1} at 0.5 and 1.0 A g^{-1}, respectively).

The increasing demand for high performance energy storage applications makes it urgent to develop new lithium ion batteries (LIBs) which possess enhanced capacity, cyclic stability and rate capability. Transitional metal oxides (TMOs), have been considered as prominent anode materials, thanks to their high theoretical specific capacity. In this context, various anode materials with different novel structures, such as Co_3O_4, Fe_2O_3, SnO_2 and TiO_2[1–3], have dramatically been explored. Among these materials, Co_3O_4 is especially noticeable due to its ease of synthesis and relative large theoretical specific capacity (~890 mAh g^{-1})[4–6]. Nevertheless, the practical application of this material is limited by its extremely low electrical conductivity as well as the rapid capacity attenuation resulted from the volume expansion/contraction as well as materials pulverization during cycling. One effective strategy to solve these problems is to design hybrid anode materials, which can not only provide active sites but also accommodate the volume change during charging/discharging process, thus attributes to higher capacity and cycling stability.

Graphene sheets (GS), with high conductivity, excellent mechanical flexibility and ultra-high specific surface area (~2360 $m^2 g^{-1}$), is envisioned as excellent candidates for substrate materials. The unique structure as well as distinctive electrical and mechanical performance is favorable to endure the strain caused by volume change and provide a continuous electron conducting networks, thus could greatly improve the electrochemical performance of active materials[7–9]. Recently, much effort has been conducted on integration of Co_3O_4 with graphene as anode materials for LIBs[10,11]. For example, Co_3O_4/graphene nanoflowers has been synthesized through a two-step process[12], involving a hydrothermal reaction of $Co(NO_3)_2{\cdot}6H_2O$ and CTAB with graphene oxide (GO) followed by a calcination. The reversible capacity of the as-synthesized composites is as high as 1120.8 mAh g^{-1} at 1 A g^{-1}. Wu *et al*. employed a surfactant-assisted hydrothermal route to synthesize Co_3O_4/nitrogen-doped graphene, within which Co_3O_4 nanoparticles with size of ~15 nm homogeneous distributed in the macropore-walls formed by graphene. The obtained composites showed excellent electrochemical performance[13]. Yang *et al*. reported the preparation of porous Co_3O_4 nanofibers coated with graphene layer, which delivers a capacity of 900 mAh g^{-1} at 1A g^{-1}[14]. These results demonstrated the integration of graphene with Co_3O_4 can remarkably improve the electrical conductivity and alleviate the volume changes of Co_3O_4 during charge/discharge reactions, thus significantly enhanced the electrochemical performance. Even though, most Co_3O_4/graphene composites are powder materials, which need a complex slurry coating process in the conventional electrode preparation method. Moreover, the electrochemical-inactive polymer binder and carbon black are required to prepare electrodes, which would increase the extra weight and decrease the energy density of the actual battery[15,16].

[1]College of Materials Science and Engineering, Chongqing University, Chongqing, 400044, China. [2]College of Aerospace Engineering, and The State Key Laboratory of Mechanical Transmissions, Chongqing University, Chongqing, 400044, China. [3]School of Chemistry and Materials Engineering, Chizhou University, Chizhou, 247000, China. [4]Key Laboratory of Low-grade Energy Utilization Technologies and Systems of the Ministry of Education of China, Chongqing, 400044, China. Correspondence and requests for materials should be addressed to R.W. (email: wangrh@cqu.edu.cn) or C.X. (email: xche@cqu.edu.cn)

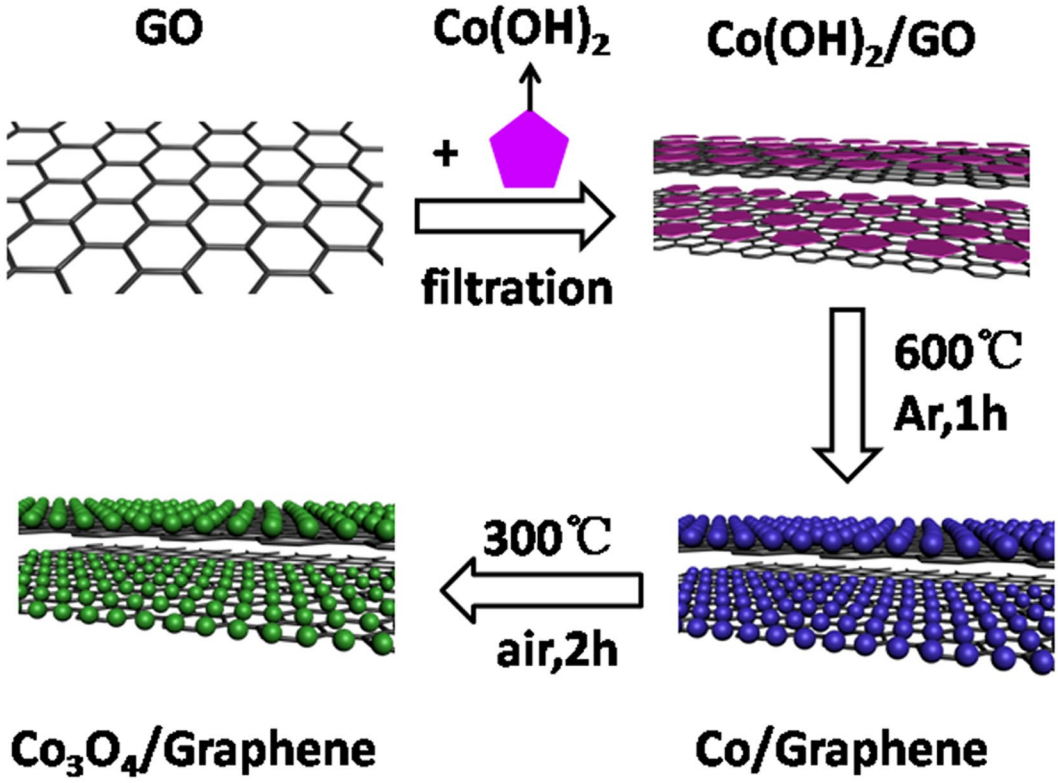

Figure 1. The fabrication process of the self-supporting Co_3O_4/GS hybrid film.

Herein, we report the synthesis of a self-supporting Co_3O_4/graphene hybrid film, which was directly used as anode materials for LIBs without any binder or additives. Co_3O_4 nanoparticles (40~60 nm) *in-situ* grew on the surface of GS, forming a novel interleaved structure with strong interfacial interactions. The hybrid electrode showed extremely high reversible capacity (1287.7 mAh g^{-1} at 0.2 A g^{-1}), good cycling stability (capacity retention of 85.5% after 100 cycles) and excellent rate capability, owing to the fascinating microstructure and binder-free electrode nature, demonstrating great potential to be used in energy storage filed.

Results

Figure 1 displayed the synthesis process of Co_3O_4/GS hybrid films. The surface of GO, functionalized with oxygen-containing functional groups[17], was measured to be a negatively charged surface (zeta potential: −60 mV) in this study. $Co(OH)_2$ colloid, which was tested to be with a zeta potential of +22 mV, was a positively charged dispersion with high stability. Learning from colloid science, there are strong electrostatic attractive interactions between two colloid with opposite charges. As a result, a flocculent solution was produced immediately when mixing GO colloid with $Co(OH)_2$ colloid, indicating an excellent self-assembly of the two dispersions driven by the strong electrostatic attractive interaction[18]. Afterwards, the flocculent solution can be easily vacuum-filtrated to construct a self-supporting $Co(OH)_2$/GO hybrid film. Further two-step heat treatments will lead to the construction of a porous and free-standing Co_3O_4/GS hybrid film which can be used as anode electrode directly.

XRD was employed to characterize the phase transformation of Co_3O_4 during preparation procedures. As shown in XRD pattern of $Co(OH)_2$/GO hybrid films (Figure 2a), the well-defined diffraction peaks can be successfully indexed to hexagonal β-$Co(OH)_2$ (JCPDS no. 74–1057). No obvious peaks of GO were detected, because graphene oxide sheets were highly separated by $Co(OH)_2$ nanosheets. After annealed in Ar atmosphere at 600 °C for 1 h, $Co(OH)_2$/GO was first converted to Co/GS as shown in Figure 2b, in which three main XRD peaks can be well assigned to Co phase (JCPDS no. 15–0806). Noteworthy, there are also no peaks of GS been detected, indicating graphene sheets were well dispersed without any aggregation. After the second step oxidation, clearly, Co phase was successfully transformed to face-centered cubic Co_3O_4 (Figure 2c, JCPDS no. 42–1467). No impurity peaks were observed, which manifests that the $Co(OH)_2$ was completely transformed to pure Co_3O_4 via a two-step heat treatments. The absence of peaks for GS suggest that graphene maintained the highly dispersibility and the restacking of graphene was well controlled during the whole preparation.

The chemical changes from precursors to Co_3O_4/GS hybrid films were analyzed by FTIR spectra. As displayed in the FTIR spectrum of $Co(OH)_2$/GO (Figure 3a), the visible peaks at about 3437, 1640 and 1077 cm^{-1} correspond to the stretching vibration of -OH in water, stretching vibration of C=C and C-O, respectively, while the peak locating at 1390 cm^{-1} represents the bending vibration of C-OH[19,20]. Apart from these characteristic peaks of oxygen functional groups originating from GO[19,20], the spectrum of $Co(OH)_2$/GO also exhibited stretching vibrations bands of Co-O bond centered at 489.8 cm^{-1} and O-OH bond in $Co(OH)_2$ (~3631 cm^{-1})[21,22]. After thermal treatment, the intensities of peaks belonging to oxygen-containing functional groups significantly decreased for

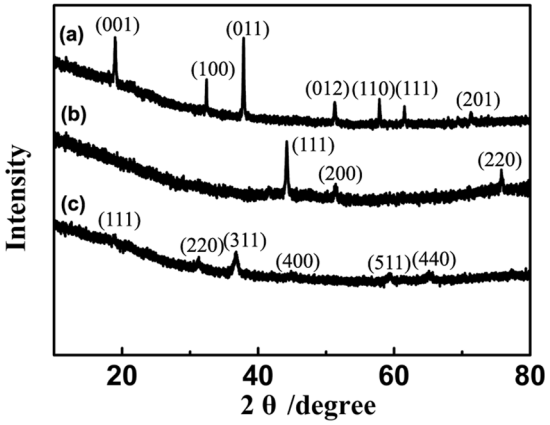

Figure 2. XRD patterns of the hybrid films: (**a**) $Co(OH)_2$/GO, (**b**) Co/GS, (**c**) Co_3O_4/GS hybrid films.

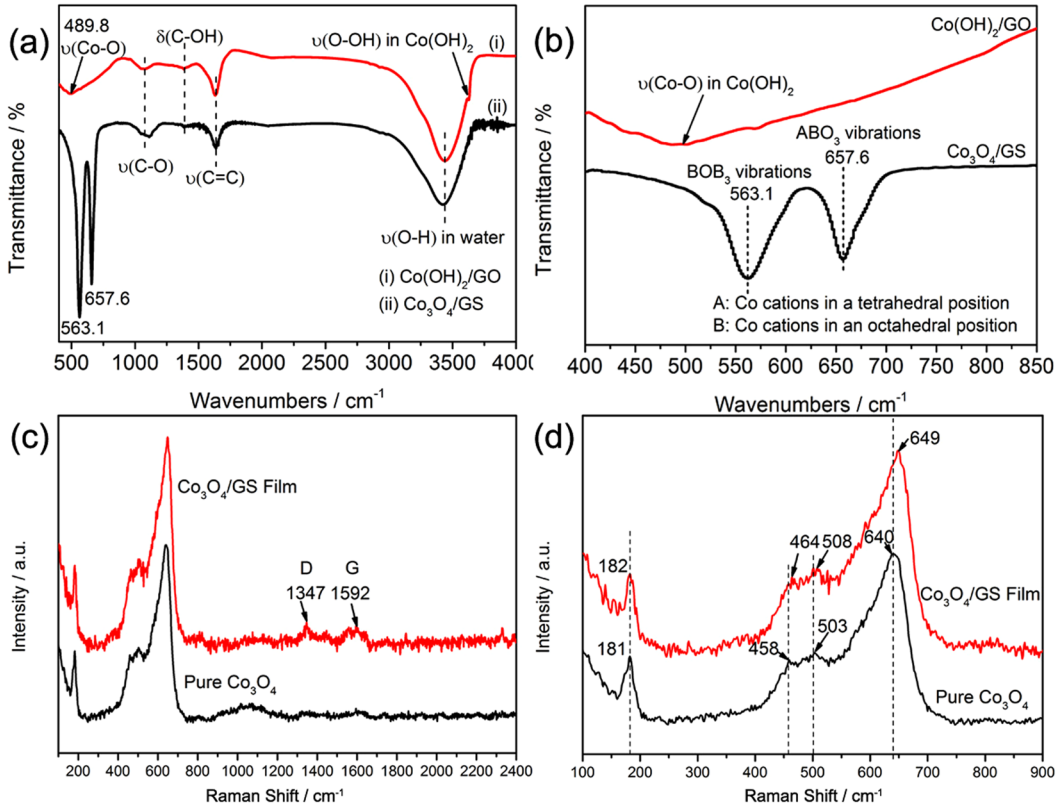

Figure 3. (**a**) FTIR spectra and (**b**) the enlarged spectra of $Co(OH)_2$/GO and Co_3O_4/GS hybrid films. (**c**) Raman spectra and (**d**) the enlarged Raman spectra of pure Co_3O_4 and Co_3O_4/GS hybrid films.

Co_3O_4/GS, suggesting the effective reduction of GO due to the thermal decomposition of these oxygen-containing functional group[23,24]. Meanwhile, the characteristic peak of υ(O-OH) in $Co(OH)_2$ disappeared, instead with two distinctive peaks appeared at 563.1 and 657.6 cm^{-1}, respectively. The first band υ1 at 563.1 cm^{-1}corresponds to the BOB_3 vibrations in the spinel lattice, in which B is associated with the Co cations in an octahedral position, i.e. Co^{3+} ions[4,8,10,25]. The second bands υ2 at 657.6 cm^{-1} is resulted from the ABO_3 vibrations (A: the metal ions in a tetrahedral position). These two stretching band can be well assigned to the characteristic peaks of Co_3O_4, further confirming the successful formation of Co_3O_4.

Figures 3c and 3d depicted the Raman spectrum of Co_3O_4 and Co_3O_4/GS composites. The three specific peaks at 458, 503 and 640 cm^{-1} can be assigned to E_g, $F_{2g}{}^1$ and $A_g{}^1$ vibration modes of pristine Co_3O_4, respectively[26,27]. While the spectrum of Co_3O_4/GS displayed two distinctive peaks at 1347 and 1592 cm^{-1} apart from those for Co_3O_4, corresponding to the D and G band of graphene[28,29], respectively. This further proves the successful preparation of Co_3O_4/GS composites, in accordance with the XRD and FTIR results. As shown in Figure 3d, the enlarged Raman spectra, the characteristic peaks representing Co_3O_4 adsorption bands in the hybrid film showed

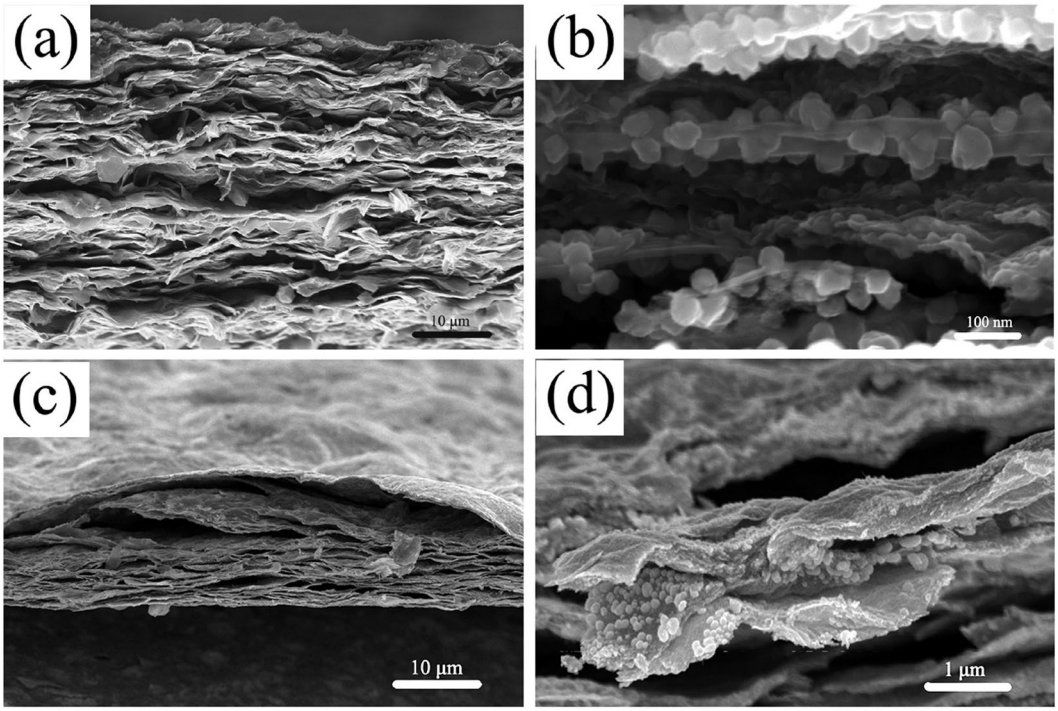

Figure 4. Cross-sectional SEM images: (**a**,**b**) Co/GS film; (**c**,**d**) Co_3O_4/GS film.

significant blue shifts compared with those of pure Co_3O_4. This suggests that there are significant interfacial interactions between Co_3O_4 and graphene within Co_3O_4/GS hybrid films, which would greatly influence the interfacial lithium ion and electron transport.

The microstructures of the hybrid films were illustrated by SEM. The as synthesized $Co(OH)_2$ shows a sheet-like morphology and will be well dispersed on the matrix of GO via electrostatic attractive force (Figure S1)[22]. After vacuum-filtration, a free-standing hybrid film with a compact layer-by-layer structure was obtained subsequently(shown in Figure S2). Interestingly, after annealing at 600 °C in Ar for 1 h, $Co(OH)_2$ nanosheets firstly decomposed and then *in-situ* reduced to cobalt nanoparticles instead of nanosheets (Figure 4a and 4b). More importantly, Co nanoparticles tightly and uniformly decorated on both surface sides of GS, suggesting strong interfacial interactions, presumably covalent bond, have formed between them. The cobalt was further *in-situ* transformed to Co_3O_4 nanoparticles with size of 40~60 nm via oxidation treatment, bringing in a self-supporting film with a porous interleaved structure (Figure 4c and 4d). The diameter of the hybrid film was about 38 mm (Figure S3), with a thickness of ~10μm (Figure 4c). The novel interleaved porous structure of Co_3O_4/GS hybrid film will greatly facilitate fast Li-ion diffusion within the electrode, and also supply abundant buffer space to allow the volume expansion of Co_3O_4 during charge/discharge processes.

Discussion

The hybrid film was directly used as electrodes, in which no polymer binder or carbon additives was added. Figure 5 illustrates the electrochemical properties of the binder-free Co_3O_4/GS hybrid electrode. As shown in the CV curves, a strong cathodic peak at about 0.6 V is observed in the first discharge process, corresponding to the multi-step electrochemical reduction between Li ions and Co_3O_4. Two anodic peaks appeared at ~1.5 and 2.3 V, owing to the oxidation of Co atoms and in consistent with the reported literatures[30,31]. The reactions can be described as:

$$Co_3O_4 + 8Li^+ + 8e^- \rightarrow 3Co + 4Li_2O \quad (1)$$

$$Co + Li_2O \rightarrow 2Li^+ + CoO + 2e^- \quad (2)$$

In the subsequent cycles, the cathodic peaks shifted to ~0.75 V, showing a tendency toward stabilization. The anodic peaks were almost the same and overlapped together, indicating the good electrochemical reversibility of the hybrid electrode.

The lithium-storage performance of the binder-free Co_3O_4/GS film was characterized by galvanostatic charge/discharge at 0.2 A g^{-1} (Figure 5b). In the discharge curve of first cycle, the potential quickly falls to a long potential plateau at ~1.5 V and then gradually decreased to 0.01 V (the cutoff voltage), which is in analogy with the behavior of Co_3O_4 anode. The first discharge/charge capacities reached 1718.5 and 1287.7 mAh g^{-1}, respectively, corresponding to the initial coulombic efficiency (CE) of 74.9%, which was comparable to that of Co_3O_4/graphene hybrid electrodes reported previously[12,32]. The relative low initial CE value may be ascribed to the inevitable

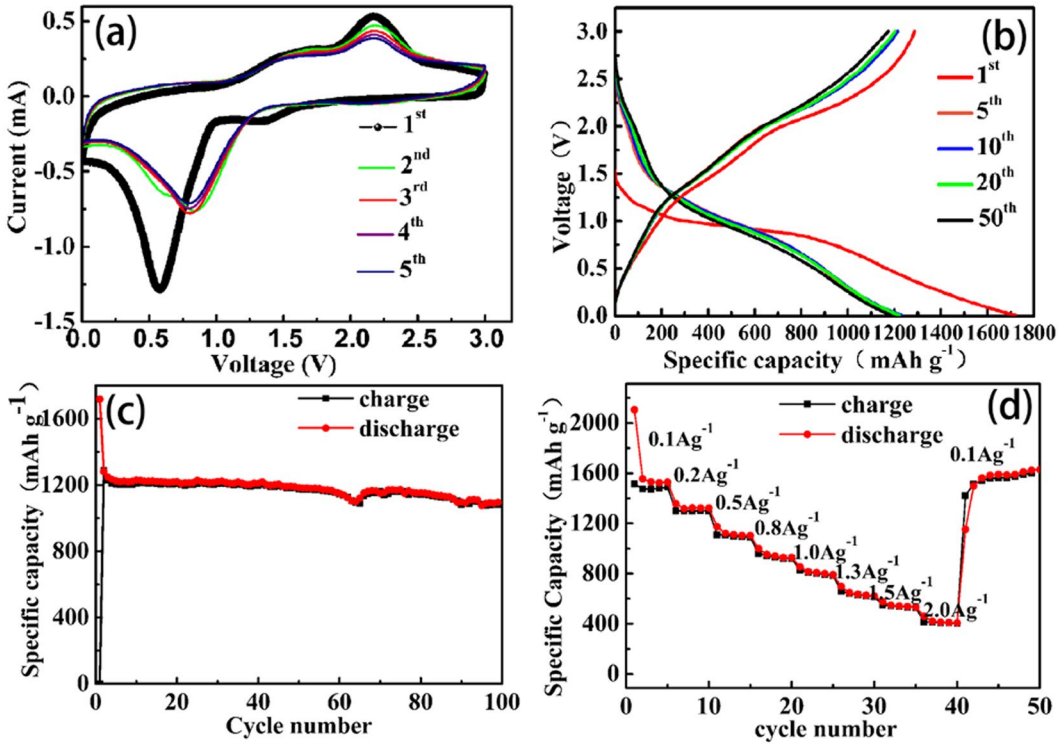

Figure 5. (**a**) Cyclic voltammograms of Co_3O_4/GS at 0.5 mVs^{-1}; (**b**) Charge/discharge voltage profiles and (**c**) Cycling performance of Co_3O_4/GS at a current density of 0.2 A g^{-1}; (**d**) Rate capability of Co_3O_4/GS hybrid film.

Electrode Material	Capacityretention	Specific capacity (mA h g^{-1})	Reference
Co_3O_4/Graphene	85.5% (0.2 A g^{-1}, 100th cycle)	800 (1 A g^{-1})	This work
Co_3O_4/nitrogen doped graphene	67% (0.1 A g^{-1}, 200th cycle)	700 (1 A g^{-1})	Ref.[13]
Sandwich-like Co_3O_4/Graphene	85.3% (0.2 A g^{-1},100th cycle)	899.8 (1 A g^{-1})	Ref.[32]
Graphene/Co_3O_4 nanotubes	89% (0.1 A g^{-1}, 80th cycle)	~600 (0.8 A g^{-1})	Ref.[34]
Plasma-treated Co_3O_4/graphene	75% (0.125 A g^{-1}, 50th cycle)	400 (0.95 A g^{-1})	Ref.[37]
Co_3O_4/CC@Graphene	39% (0.1 A g^{-1}, 100th cycle)	469(0.05 A g^{-1})	Ref.[38]
Co_3O_4–graphene sheet-on-sheet	76% (0.1 A g^{-1}, 50th cycle)	~400 (0.8 A g^{-1})	Ref.[39]

Table 1. Comparison of electrochemical performance of anode materials based on Co_3O_4 and graphene.

formation of a solid electrolyte interface (SEI) film over the electrode during the charge/discharge process, which led to the insufficient release of capacity. A well-established conductive network may help to further increase the CE[32], such as surface modification[13], pre-doping lithium metal[33] and encapsulation[34]. Compared with the theoretical capacity of graphene (372 mAhg^{-1}) and Co_3O_4 (890 mAh g^{-1}), the extra capacity may owe to the formation of SEI film or interfacial Li-ion storage[35,36]. After fifty charge/discharge cycles, the discharge capacity still remains up to 1184.2 mAh g^{-1}, demonstrating the good structural stability of the Co_3O_4/graphene anode.

Figure 5c highlights the cycling stability of the Co_3O_4/GS anode at 0.2 A g^{-1}. The hybrid anode retains a reversible capacity of 1095.1 mAhg^{-1} after 100 cycles with the capacity retention of 85.5%. The rate capacity of the self-supported Co_3O_4/GS electrode has also been studied in Figure 5d. The capacities of Co_3O_4/GS heterostructures were about 1480, 1300, 1110, 920, 800, 620, 530 and 410 mAh g^{-1} at the current densities of 0.1, 0.2, 0.5, 0.8, 1.0, 1.3, 1.5 and 2.0 A g^{-1}, respectively, manifesting an excellent rate capability. Importantly, the capacity re-increased to 1601.2 mAh g^{-1} when the current density returns back to 0.1 A g^{-1}, further demonstrating the good reversibility. Compared with the capacities and cycling performance of other Co_3O_4-based anode materials reported previously (shown in Table 1), the constructedCo_3O_4/GS anode exhibited higher capacity and better stability than Co_3O_4/nitrogen doped graphene[13], graphene/Co_3O_4 nanotubes[34], plasma treated Co_3O_4/Graphene[37], Co_3O_4/CC@graphene[38], Co_3O_4/graphene sheet on sheet[39] and so on. For the as-prepared Co_3O_4/GS hybrid film, the strong interfacial interactions between Co_3O_4 and GS can greatly facilitate the interfacial charges transportations, which is beneficial to enhance the lithium-storage capacity at high current densities. In addition, more active sites were achieved owing to the small particle size of Co_3O_4 and porous interleaved structure, accounting for the enhanced capacity. The flexible graphene substrate and porous structure, can provide buffer space for volume change of Co_3O_4 nanoparticles and effectively prevent their aggregation, which contributes to the excellent

cycling stability. Overall, the Co_3O_4/GS hybrid film delivered superior electrochemical performance benefitting from the synergistic effects of strong interfacial interactions between Co_3O_4 and graphene, small particle size of Co_3O_4, the interleaved porous structure and binder-free electrode nature, suggesting the superiority of using the hybrid films as an anode material for LIBs. Moreover, the two-step fabrication process is simple, controllable and low-cost, showing great promise to be used in practical applications

Conclusion

In summary, a vacuum filtration procedure combined with two-step heat treatment has been developed to construct self-supporting Co_3O_4/GS hybrid films, with Co_3O_4 nanoparticles (40–60 nm) uniformly and tightly decorated on both surface of GS. The formed porous and interleaved microstructure exhibits critical characters as desired anode materials for LIBs, such as strong interfacial interactions, short transport length for Li-ion, and sufficient space for stress relaxation. Consequently, the constructed Co_3O_4/GS hybrid film as binder-free electrode exhibited a high capacity of 1287.7 mAh g^{-1} at 0.2 A g^{-1}, good cycling stability (capacity retention of 85.5% after 100 cycles at 0.2 A g^{-1}) and superior rate capability, making the hybrid films competitive as LIBs anode materials.

Materials and Methods

β-$Co(OH)_2$ was synthesized based on previous report and further diluted to a homogeneous dispersion (0.5 mg mL^{-1})[40,41]. Graphene oxide (GO) was prepared using a modified Hummers method with natural graphite as raw materials[42], which was also diluted to 0.5 mg mL^{-1} for further use.

For preparation of Co_3O_4/GS film, the β-$Co(OH)_2$ and GO dispersion were mixed together by sonication; and then vacuum filtered to form a self-supporting $Co(OH)_2$/GO hybrid film. Afterwards, two-step heat treatment approach was carried out: First, the obtained $Co(OH)_2$/GO film was heat-treated in Ar at 600 °C for 1 h to produce Co/GS. Second, Co/GS was further oxidized to Co_3O_4/GS by being calcined in air (300 °C, 2 h).

Materials Characterizations. The morphologies and microstructures of the samples were characterized via field-emission scanning electron microscopy(FE-SEMJSM-6700F). The crystalline phase of the materials was analyzed from X-ray diffraction measurements (Rigaku D/max 2550 V diffractometer). Raman spectroscopy was conducted on DXR Raman Microscope (Thermal Scientific Corporation, USA, wavelength 532 nm). Fourier transform infrared spectroscopy (FTIR) were examined on Nicolet 7000-C.

Electrochemical Measurements. In this paper, the as-synthesized self-supporting Co_3O_4/GS hybrid films were directly used as an electrode without adding any binder or additive. The cell was assembled in glove box, and Li foil was adopted as the counter electrode. The 1 M $LiPF_6$ in a mixture of ethylene carbonate (EC)/dimethyl carbonate (DMC)(50:50, by volume) was used as electrolyte. The electrochemical properties were measured using a CT2001 battery tester at room temperature. Cyclic voltammetry (CV) was performed via electrochemical workstation (CHI760E) at a scan rate of 0.5 mV s^{-1} within a voltage range of 0–3.0 V. The mass loading was about 0.8 mg for each Co_3O_4/GS electrode.

References

1. Reddy, M. V., Subba Rao, G. V. & Chowdari, B. V. R. Metal Oxides and Oxysalts as Anode Materials for Li Ion Batteries. *Chem. Rev.* **113**, 5364–5457 (2013).
2. Wang, Z. Y., Zhou, L. & Lou, X. W. Metal Oxide Hollow Nanostructures for Lithium-ion Batteries. *Adv. Mater.* **24**, 1903–1911 (2012).
3. Xu, C. H., Sun, J. & Gao, L. Controllable synthesis of monodisperse ultrathin SnO_2 nanorods on nitrogen-doped graphene and its ultrahigh lithium storage properties. *Nanoscale* **4**, 5425–5430 (2012).
4. Wu, Z. S. *et al.* Graphene Anchored with Co_3O_4 Nanoparticles as Anode of Lithium Ion Batteries with Enhanced Reversible Capacity and Cyclic Performance. *Acs Nano* **4**, 3187–3194 (2010).
5. Xia, X. H. *et al.* Self-supported hydrothermal synthesized hollow Co_3O_4 nanowire arrays with high supercapacitor capacitance. *J. Mater. Chem.* **21**, 9319–9325 (2011).
6. Xia, X. H., Tu, J. P., Wang, X. L., Gu, C. D. & Zhao, X. B. Mesoporous Co_3O_4 monolayer hollow-sphere array as electrochemical pseudocapacitor material. *Chem. Commun.* **47**, 5786–5788 (2011).
7. Kim, H., Seo, D. H., Kim, S. W., Kim, J. & Kang, K. Highly reversible Co_3O_4/graphene hybrid anode for lithium rechargeable batteries. *Carbon* **49**, 326–332 (2011).
8. Li, B. J. *et al.* Co_3O_4@graphene Composites as Anode Materials for High-Performance Lithium Ion Batteries. *Inorg. Chem.* **50**, 1628–1632 (2011).
9. Xu, C., Wang, X., Zhu, J. W., Yang, X. J. & Lu, L. Deposition of Co_3O_4 nanoparticles onto exfoliated graphite oxide sheets. *J. Mater. Chem.* **18**, 5625–5629 (2008).
10. Yuan, C. *et al.* Flexible Hybrid Paper Made of Monolayer Co_3O_4 Microsphere Arrays on rGO/CNTs and Their Application in Electrochemical Capacitors. *Adv. Funct. Mater.* **22**, 2560–2566 (2012).
11. Zhao, X., Hayner, C. M., Kung, M. C. & Kung, H. H. In-Plane Vacancy-Enabled High-Power Si-Graphene Composite Electrode for Lithium-IonBatteries. *Adv. Energy. Mater.* **1**, 1079–1084 (2011).
12. Jiang, Y. *et al.* Co_3O_4-graphene nanoflowers as anode for advanced lithium ion batteries with enhanced rate capability. *J. Alloys Compd.* **710**, 114–120 (2017).
13. Xing, X. *et al.* Surfactant-Assisted Hydrothermal Synthesis of Cobalt Oxide/Nitrogen-Doped Graphene Framework for Enhanced Anodic Performance in Lithium Ion Batteries. *Electrochim. Acta.* **194**, 310–316 (2016).
14. Hu, R. *et al.* Porous Co_3O_4 nanofibers surface-modified by reduced graphene oxide as a durable, high-rate anode for lithium ion battery. *Electrochim. Acta* **228**, 241–250 (2017).
15. Yao, Z. *et al.* Hybrid vertical graphene/lithium titanate–CNTs arrays for lithium ion storage with extraordinary performance. *J. Mater. Chem. A* **5**, 8916–8921 (2017).
16. Zhou, C. A. *et al.* Rational construction of a metal core for smart combination with $Li_4Ti_5O_{12}$ as integrated arrays with superior high-rate Li-ion storage performance. *J. Mater. Chem.* **A5**, 1394–1399 (2017).
17. Wang, R., Xu, C., Sun, J., Gao, L. & Lin, C. Flexible free-standing hollow Fe_3O_4/graphene hybrid films for lithium-ion batteries. *J. Mater. Chem. A* **1**, 1794–1800 (2013).
18. Xu, C. *et al.* Electronic Coupling of Cobalt Nanoparticles to Nitrogen-Doped Graphene for Oxygen Reduction and Evolution Reactions. *Chem Sus Chem* **9**, 3067–3073 (2016).

19. Li, D., Muller, M. B., Gilje, S., Kaner, R. B. & Wallace, G. G. Processable aqueous dispersions of graphene nanosheets. *Nat. Nanotechnol.* **3**, 101–105 (2008).
20. Pei, S. F. & Cheng, H. M. The reduction of graphene oxide. *Carbon* **50**, 3210–3228 (2012).
21. Zhao, T., Jiang, H. & Ma, J. Surfactant-assisted electrochemical deposition of alpha-cobalt hydroxide for supercapacitors. *J. Power Sources* **196**, 860–864 (2011).
22. Wang, R. *et al*. Free-standing and binder-free lithium-ion electrodes based on robust layered assembly of graphene and Co_3O_4 nanosheets. *Nanoscale* **5**, 6960–6967 (2013).
23. Lee, J. Y. *et al*. Sea-Urchin-Inspired 3D Crumpled Graphene Balls Using Simultaneous Etching and Reduction Process for High-Density Capacitive Energy Storage. *Adv. Funct. Mater.* **25**, 3606–3614 (2015).
24. Lei, Z., Lu, L. & Zhao, X. S. The electrocapacitive properties of graphene oxide reduced by urea. *Energy Environ. Sci.* **5**, 6391–6399 (2012).
25. Chen, S. Q. & Wang, Y. Microwave-assisted synthesis of a Co_3O_4-graphene sheet-on-sheet nanocomposite as a superior anode material for Li-ion batteries. *J. Mater. Chem.* **20**, 9735–9739 (2010).
26. Wang, G. X. *et al*. Hydrothermal Synthesis and Optical, Magnetic, and Supercapacitance Properties of Nanoporous Cobalt Oxide Nanorods. *J. Phys. Chem.* **C113**, 4357–4361 (2009).
27. Xiong, S. L., Yuan, C. Z., Zhang, M. F., Xi, B. J. & Qian, Y. T. Controllable Synthesis of Mesoporous Co_3O_4 Nanostructures with Tunable Morphology for Application in Supercapacitors. *Chem.Eur. J.* **15**, 5320–5326 (2009).
28. Beams, R., Cancado, L. G. & Novotny, L. Raman characterization of defects and dopants in graphene. *J.Phys.:Condens.Matter* **27**, 083002 (2015).
29. Paton, K. R. *et al*. Scalable production of large quantities of defect-free few-layer graphene by shear exfoliation in liquids. *Nat. Mater*. 624–630 (2014).
30. Qiu, D. *et al*. *In situ* growth of mesoporous Co_3O_4 nanoparticles on graphene as a high-performance anode material for lithium-ion batteries. *Mater. Lett.* **119**, 12–15 (2014).
31. Wang, Q., Zhang, C.-Y., Xia, X.-B., Xing, L.-L. & Xue, X.-Y. Extremely high capacity and stability of Co_3O_4/graphene nanocomposites as the anode of lithium-ion battery. *Mater. Lett.* **112**, 162–164 (2013).
32. Yang, Y., Huang, J., Zeng, J., Xiong, J. & Zhao, J. Direct Electrophoretic Deposition of Binder-Free Co_3O_4/Graphene Sandwich-Like Hybrid Electrode as Remarkable Lithium Ion Battery Anode. *ACS Appl. Mater. Interfaces* **9**, 32801–32811 (2017).
33. Seong, I. W., Kim, K. T. & Yoon, W. Y. Electrochemical behavior of a lithium-pre-doped carbon-coated silicon monoxide anode cell. *J. Power Sources* **189**, 511–514 (2009).
34. Li, D. *et al*. Graphene membrane encapsulated Co_3O_4 nanotubes with superior capacity and stability as anode materials for lithium ion batteries. *J. Sol-Gel Sci. Technol.* **82**, 75–84 (2016).
35. Xiong, S. L., Chen, J. S., Lou, X. W. & Zeng, H. C. Mesoporous Co_3O_4 and CoO@C Topotactically Transformed from Chrysanthemum-like $Co(CO_3)_{0.5}(OH)$center dot $0.11H_2O$ and Their Lithium-Storage Properties. *Adv. Funct. Mater.* **22**, 861–871 (2012).
36. Lou, X. W., Deng, D., Lee, J. Y., Feng, J. & Archer, L. A. Self-supported formatnion of needlelike Co_3O_4 nanotubes and their application as lithium-ion battery electrodes. *Adv. Mater.* **20**, 258–262 (2008).
37. Long, H. *et al*. Plasma-treated Co_3O_4/graphene nanocomposite as high performance anode of lithium-ion battery. *J. Alloys Compd.* **701**, 200–207 (2017).
38. Zhao, Q. X. Y. Z. Y. Z. W. F. X. Z. P. Graphene enhanced anchoring of nanosized Co_3O_4 particles on carbon fiber cloth as free-standing anode for lithium-ion batteries with superior cycling stability. *Electrochim. Acta* **247**, 125–131 (2017).
39. Su, Q. *et al*. Microwave-assisted synthesis of Co_3O_4–graphene sheet-on-sheet nanocomposites and electrochemical performances for lithium ion batteries. *Mater. Res. Bull.* **72**, 43–49 (2015).
40. Wang, R. *et al*. Controllable synthesis of nano-$LiFePO_4$ on graphene using Fe_2O_3 precursor for high performance lithium ion batteries. *Mater. Lett.* **112**, 207–210 (2013).
41. Xu, C. H., Sun, J. & Gao, L. Direct growth of monodisperse SnO_2 nanorods on graphene as high capacity anode materials for lithium ion batteries. *J. Mater. Chem.* **22**, 975–979 (2012).
42. Zhao, Y. *et al*. Functional graphene nanomesh foam. *Energy Environ. Sci.* **7**, 1913–1918 (2014).

Acknowledgements

This work is financially supported by the National Natural Science Foundation of China (21503025, 21603019), Fundamental Research Funds for the Central Universities (0903005203377, 106112016CDJXY130001, 106112016CDJZR325520), Educational Commission of Anhui Province of China (KJ2014A176), Chongqing Research Program of Basic Research and Frontier Technology (cstc2016jcyjA1059), and Hundred Talents Program at Chongqing University.

Author Contributions

Chaohe Xu and Ronghua Wang conceived the idea, designed the research, proposed the conceptual idea and provided the financial support. Shouling Wang and Jie Chang performed materials characterization, electrochemical test and data analysis. All authors participated in discussing, writing and approving the final manuscript.

Additional Information

Supplementary information accompanies this paper at https://doi.org/10.1038/s41598-018-21436-4.

Competing Interests: The authors declare no competing interests.

Publisher's note: Springer Nature remains neutral with regard to jurisdictional claims in published maps and institutional affiliations.